CHAPTER 3
THE TELESCOPE, RECEIVER SYSTEM AND THE SPECTRAL LINE BACK-END

The observations reported in this thesis were carried out using the Ooty Radio Telescope (ORT). These observations made over a period of 3 years constitute the first major spectral line study using the ORT. The observational program involved building, installing and testing of several new items of equipment and associated computer software development to make the ORT suitable for spectral line observations. In this chapter we describe and discuss some of the instruments.

The charactersitics of the ORT as designed and built more than 15 years ago have been described in several papers (Swarup et al 1971, Sarma et al 1975a, 1975b, Kapahi et al 1975, Ananthakrishnan 1976). Since then, the ORT has undergone several modifications and improvements due to the continuing and dedicated efforts of the staff of the Radio Astronomy Centre at Ooty. We begin here with a brief description of the ORT and its receiver system as it existed during the period of these observations.

3.1 THE ANTENNA

The ORT is a 530m x 30m parabolic cylinder with its axis along the north-sourth direction situated at a latitude of $11^{\circ}\ 23'$. One of the interesting aspects of this telescope is that its axis has been made parallel to the earth's axis of rotation by building it on a hill slope inclined at an angle of $\sim 11^{\circ}$ to the horizontal. As a result, any celestial source can be tracked during its diurnal motion by a simple rotation of the ORT about its axis at a fixed speed. At its nominal operating centre frequency of 326.5MHz the ORT has a half power beam width of

$5'.6 \sec\delta$ in the north-south direction and 2° in the east-west direction. The declination range is approximately $\pm 35^\circ$ and within it the telescope can track any source from hour angle -4^h07^m to 5^h26^m, amouting to a continuous tracking time of about 9.5 hours.

The feed system of the ORT consists of 1056 dipoles mounted below a corner reflector along the focal line of the parabolic cylinder. The 1056 dipoles are divided into 22 modules of 48 dipoles each. Starting from the middle of the telescope the northern modules are designated as N1, N2.. ..N11, and the southern modules as S1, S2, ... S11. The 48 dipoles of each module are connected in a christmas tree fashion with a 4-bit diode phase shifter in series with each of the dipoles. A 192-bit control signal coming either from a computer or a manual unit (selectable by a switch), steers the primary beam of each of these modules in declination. The mid point of the 48 dipoles is used as the phase centre, and opposite phases are set in the northern and southern half of the modules to achieve a phase gradient to steer the beam in declination.

3.2 THE RECEIVER SYSTEM

The signals from each of the 22 modules are first amplified in RF amplifiers centered at 326.5MHz and having a bandwidth of ~12MHz. The noise temperature of the RF amplifiers is about 110K. The signals are then down-converted to an IF of 30MHz using a local oscillator frequency of 296.5MHz. A band pass filter having sufficient rejection (>60dB) at the image band frequency (267.5MHz) is provided between each RF amplifier and the following mixer. The RF amplifier and the mixer along with the first IF amplifier for each of the modules are situated on the antenna itself. The local oscillator is generated in the receiver room (with a power of ~6Watts) and is fed to each of the mixers through an equal length branching system using low loss cables.

A block diagram of the receiver system of the ORT is shown in fig 3.1. The 30MHz IF signals from each of the modules are brought into the receiver room for further processing using equal length cables. After compensating for the loss in these cables in the first post IF amplifier (PA1) the signals are passed through a set of delay and phase compensating cables and phase trimmers before they enter the next stage of IF amplification in PA2. The signals from each of the 22 modules at the output of the PA2 amplifiers are split equally in 12-way dividers. A test port is also provided at the output of the PA2 amplifiers for monitoring or checking of the signals from each of the modules. By diverting the signal into this test port it is'possible to cut off the signal from any one of the modules from entering the subsequent circuitry. In other words, the contribution from any of the 22 modules to the final output can be eliminated with the help of a switch.

The outputs corresponding to the 11 northern modules and the 11 southern modules are combined separately in 12 different ways in the beam forming network to give 12 pairs of 'north' and 'south' signals (N and S). These 12 pairs of signals correspond to 12 simultaneous beams in the sky with separations in declination of $3'.6/\cos\delta$ between adjacent beams. The 12 simultaneous beams which cover a span of 36 arcminutes in declination are usually used to track the moon for lunar occultation studies of radio sources.

The N and S signals corresponding to each of the 12 beams are amplified in a high gain final IF amplifier PA3. The PA3 amplifiers, which are centred at 30MHz have a nearly rectangular bandshape of width 4MHz and they determine the final bandwidth of the system; all the preceeding stages are broad band (bandwidth >12MHz). From the normal operating point (+7dbm output), the PA3 amplifiers saturate when the signal increases by about 3dB (saturation level +10dbm). Variable attenuators are provided, just before the PA3 amplifiers, to enable observations of strong sources without saturating the PA3 amplifiers.

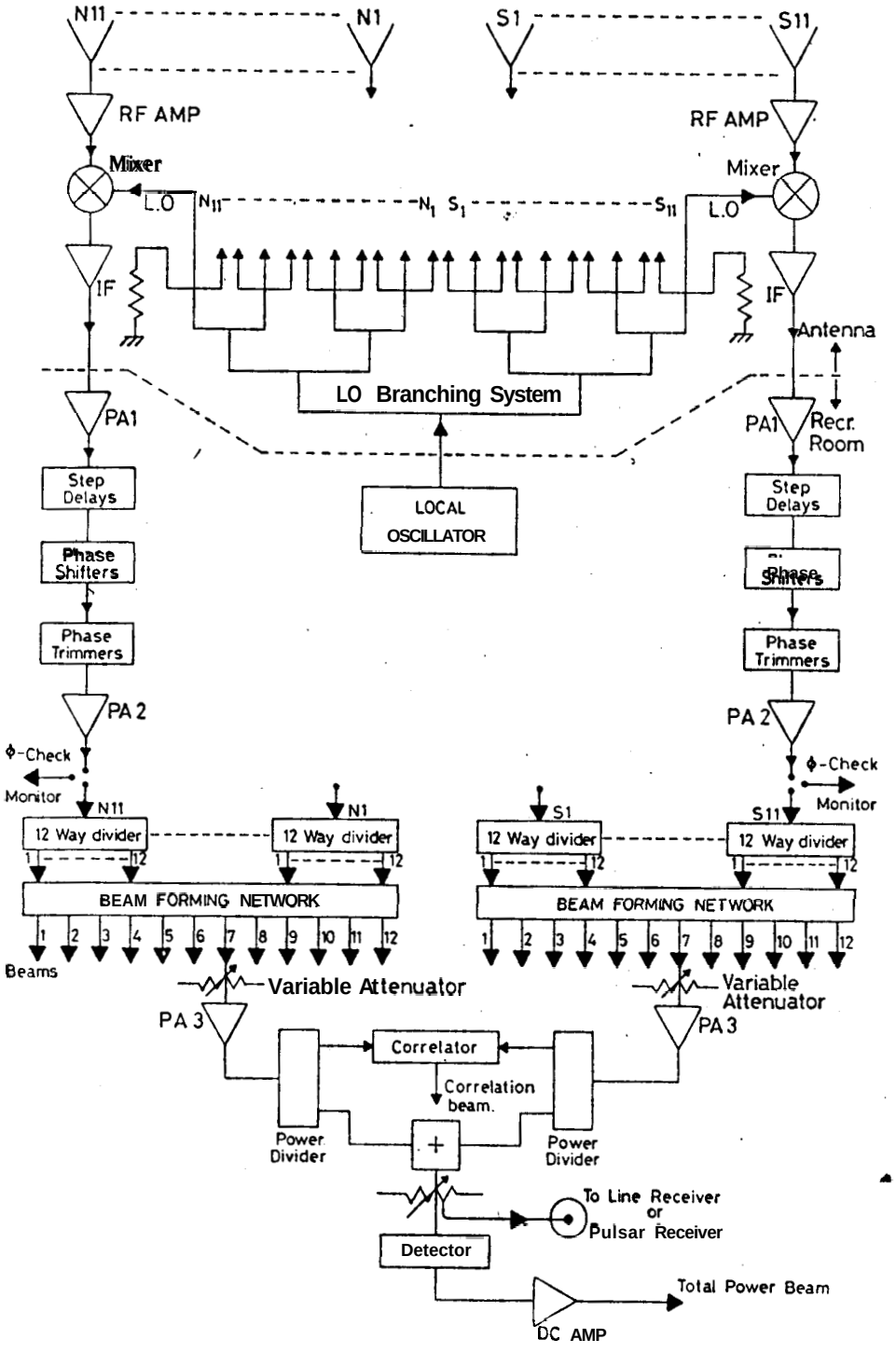

Fig. 3.1 A Block–diagram of the ORT Receiver System.

The signals from the PA3 amplifiers are further split in 2 way dividers to each ofprovide 2 pairs of N and S outputs corresponding to the 12 beams. One set of the signal pairs are multiplied to form 12 simultaneous correlated beams and the other pairs are added to form 12 total power beams. The outputs of the 12 correlated beams go to the computer (Varian 620i) through a 12 bit A/D converter and also to a 12 pen chart recorder. The 12 total power outputs after square law detection and DC amplification also go to the computer through the ADC and to the 12 pen recorder. Each of the 12 pens of the recorder can be selected to record signals from either the correlated beam or the total power beam with the help of a switch. The 12 total power outputs are also made available before detection in auxilary ports (28db down) for further processing, either in the pulsar receiver or the spectral line receiver.

Pointing the ORT beam towards a given declination is done in 2 steps. First the individual modules are steered by setting an appropriate phase gradient across the 48 dipoles using the 4-bit diode phase shifters (quantized to 22.5, 45, 90 and 180 degrees). This can be done either through computer control or by using a manual unit. The quantized phase-shifts are all at the centre frequency of 326.5MHz. Path differences of integral number of wavelengths, between the dipoles within a module are not compensated. As the final bandwidth of the system is only about 1.2% of the centre frequency and the length of each module is only $\sim 25\lambda$ the uncompensated delays for the declination range of $\pm 30^{\circ}$ causes negligible bandwith decorrelation (<5%). The next step in setting the declination is to compensate for the phases and delays between the 22 modules before combining the signals at IF. The delays are compensated at the IF (30MHz) to within $\pm 1\lambda$ using the step delay cables,. and the remaining phase is adjusted using fractional wavelengh cables (up to $\lambda/32$). The delay and phase for the IF can again be set either through computer or manual control of a set of diode switches.

The phase trimmers are used for adjusting the phase errors in the signal paths from each module. This is done by pointing

the antenna to a point source and maximising the correlation of the signal from a given module in the north nr south half of the telescope with the combined signal from the other half. The process is repeated for every module. This operation, which is called 'phasing of the telescope', is usually done once a week.

3.3 SENSITIVITY OF THE ORT

The factors which determine the sensitivity of a radio telescope are the system temperature (T_{sys}), the effective area of the telescope (A_{eff}) and the main beam efficiency (η_B). These parameters of the system are in turn dependent on several factors pertaining to the telescope and the receiver system. Some of these are listed below

1. Aperture illumination efficiency (η_{ill}) determined by the design of the feed.

2. Ground and the sky background radiation (T_{bg}) picked up by the feed determined by the spillover charecteristics of the feed.

3. Loss in the feeder system (α) connecting the dipoles to the RF amplifier.

4. Signal loss resulting from imperfect matching of the output from each module to the input of the RF amplifier (η_{Tx}).

5. Noise temperature of the RF amplifier (T_R).

6. Signal loss resulting from bandwidth decorrelation due to uncompensated delays in the system (η_{coh}).

7. Signal loss due to r.m.s amplitude and phase errors in the system due to quantized RF and IF phase shifters and errors in the cable lenghts (η_R).

3.3.1 The System Temperature

The system temperature when the antenna is pointed towards a cold region in the sky is given by (see fig 3.2a)

$$T_{sys} = T_R + \alpha T_{Bg} + (1-\alpha) T_O \qquad (3.1)$$

where

T_R = 110K the noise temperature of the RF amplifier
= 0.76 corresponding to 1.2dB loss in the RF feeder system

TO = 300K the ambient temperature

$T_{Bg} = T_{sky} + T_{ground}$ (spill over of the feed)
= 45K + 30K = 75K

For the ORT with the above values

$T_{sys} \simeq 250K$

The r.m.s. noise at the output of the receiver is given by

$$\Delta T_{rms} = \frac{K \cdot T_{sys}}{\sqrt{B \cdot \tau}}$$

where B is the final bandwidth of the receiver system and τ is the integration time. The factor K depends on the type of the receiver used. For the correlation receiver K=1.414 and for th total power receiver K=1.0.

3.3.2 Sensitivity measurement using the correlation beam

The routine method employed for measuring the sensitivity of the ORT using the correlation beam is as follows

A list of point sources of known flux (at 327 MHz) spread over the right ascention range of 0^h-24^A and declination $\pm 25^o$, known as calibration sources, is available for making sensitivity measurements. The calibration sources have angular sizes much

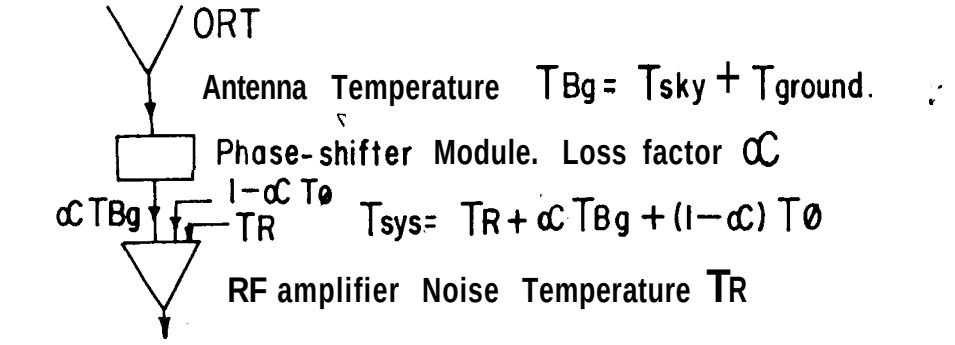

a. ORT System temperature.

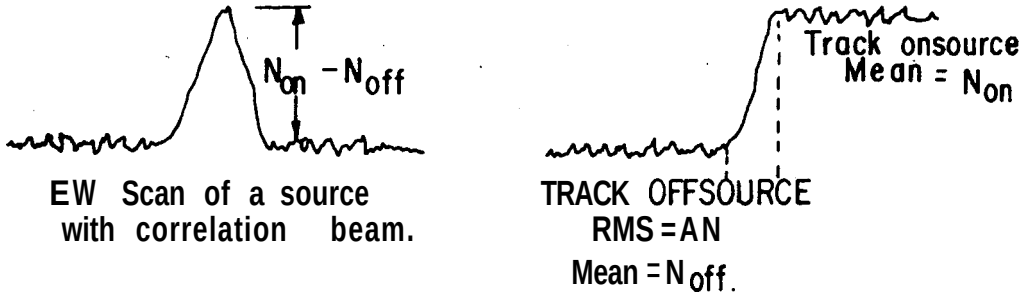

b. Sensitivity measurement with correlation beam

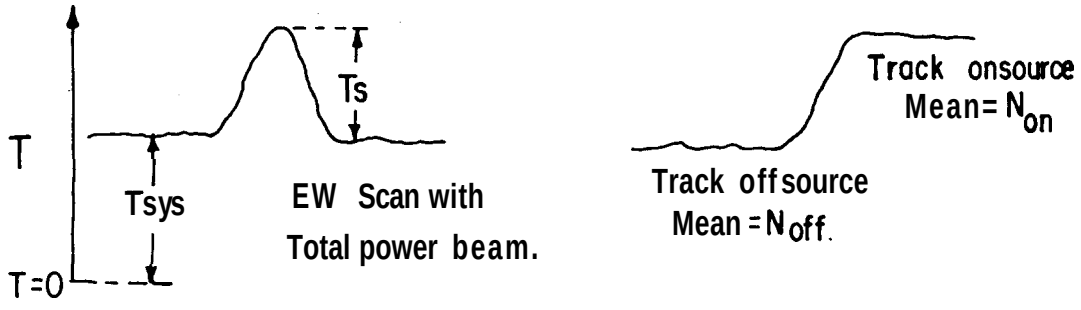

c. Sensitivity measurement with total power beam.

FIG.3.2. SYSTEM TEMPERATURE & SENSITIVITY MEASUREMENT

smaller than the ORT beam and can be considered to be point source's. Using the correlation beam one can measure the signal to noise that can be obtained for any of these calibration sources. Usually the central beam (Beam 7) is used for this purpose. The proceedure is to track an off source region at the same declination as the calibration source, but shifted in right ascention and to measure the r.m.s. noise fluctuation at the output of the receiver. This is done by sampling the digitized output from the correlator for 60 seconds using the computer, and calculating the mean (N_{off}) and r.m.s. (ΔN) of the recorded counts. The telescope is then made to track the calibration source and the mean on-source counts (N_{on}) is measured, again by sampling the output for 60 seconds. The signal to noise ratio for the source is then given by

$$\left(S/N\right) = \frac{N_{on} - N_{off}}{\Delta N}$$

A convenient unit is the signal to noise ratio per Jansky which is obtained by dividing the above quantity by the flux density of the source in Janskies (1 Jansky = 1.OE-26 $Wm^{-2} Hz^{-1}$). This measurement proceedure is indicated schematically in FIG. 3.2b. The main uncertainty in this measurement is in the accuracy of determination of the rms noise AN.

The signal to noise ratio per Jansky (s) was measured using several of the calibration sources (eg. 3C283, 3C245, 1136-13, 1453-10, 3C403, 3C195 etc). The measured value of s is usually between 8 and 10. A typical mean value is 9.

The expected r.m.s noise in the correlation beam output is given by equation 3.2. The relevant values for the bandwidth and integration times used are

B = 4MHz and τ = 1second; K = 1.414

whence

$$\Delta T_{rms} = \frac{1.414 \times 250}{\sqrt{4 \times 10^6 \times 1}} = 0.18\,K$$

If the increase in the system temperature for a 1 Jansky source is $T_{A\phi}$ then (ϕ to indicate correlation beam)

$$s = \frac{T_{A\phi}}{\Delta T_{rms}} \quad \text{or} \quad T_{A\phi} = s \times \Delta T_{rms}$$

Using a mean value for s = 9 and the values for ΔT_{rms} from above, the increase in system temperature for the correlation beam is

$$T_{A\phi} = 1.6\,K \text{ per Jansky}$$

The meaning of this number is discussed later.

3.3.3 Sensitivity Measurement Using the Total Power Beam

It is not possible to employ the same method (viz. as for the correlation beam) here to measure the sensitivity, using the existing total power(TP) set up. The advantage of the correlation beam is that the baselines are stable and it allows the measurement of the rms noise. This is because the gain fluctuations in the north and south half of the telescope which are uncorrelated do not contribute to the output. The broad variations in the off-source sky background which will be resolved out by correlation beam also do not contribute. These fluctuations contribute only to the rms noise at the output, and do not cause any baseline variation. On the other hand, the total power output continuously follows these variations. Therefore if the gain of the total power system is kept at a level so as to show the rms noise fluctuations (purely due to the T_{sys}), then the system gain and sky background variations produces a drift in the baseline which are much larger than the pure noise fluctuations and any rms noise measurement by sampling the total power output become meaningless ; it will largely reflect the baseline variations. The foregoing discussion applies when the bandwidth and the integration time used with the total power beam are similar to the correlation beam However, if one uses a much smaller bandwidth and time constant, the fluctuations at the total power output can be made to be dominated by pure noise fluctuations and not by system gain and

sky background variations. In this case very strong calibration sources are needed for the **sensititvity measurements.**

The method employed for measuring the sensitivity using the TP **beam** is to make absolute measurements of the off-source and the on-source levels at the output of the TP detector. These measurements are used along with a correction for the departure of the detector law from a true square **law** to obtain the increase in system temperature per Jansky in the TP beam (T_{Atp})

The measurement proceedure is indicated schematically in fig 3.2c. An off-source region at the same declination as a calibration source but shifted in right ascention is first tr'acked. The digitized output of the TP detector is sampled by the computer and its mean value N_{off} is computed. Usually two off-source regions on either side of the calibration source are used to measure a mean N_{off}. The mean on-source level N_{on} is then measured by tracking the calibration source. A DC offset present in both N_{off} and N_{on} due to the DC amplifier is separately measured and taken out.

The measured N_{off} corresponds to the cold sky system temperature T_{sys} and N_{on} corresponds to $(T_{sys} + T_{AS})$ where T_{AS} is the increase in the system temperature due to the source. It can be shown that

$$T_{AS} = \left[\left(\frac{N_{on}}{N_{off}} \right)^{m} - 1 \right] \times T_{sys} \qquad (3.3)$$

where m is the factor accounting for the departure of the detector from a true square law. m is in fact the slope of a plot of input power to the detector (in dB) against the output voltage (in dB) shown in fig 3.3 The measured value of m is 1.28; for a true square law detector m=1.0. The increase in system temperature per Jansky in the TP beam is then given by

$$T_{Atp} = T_{AS} / S$$

where S is the flux density of the calibration source in

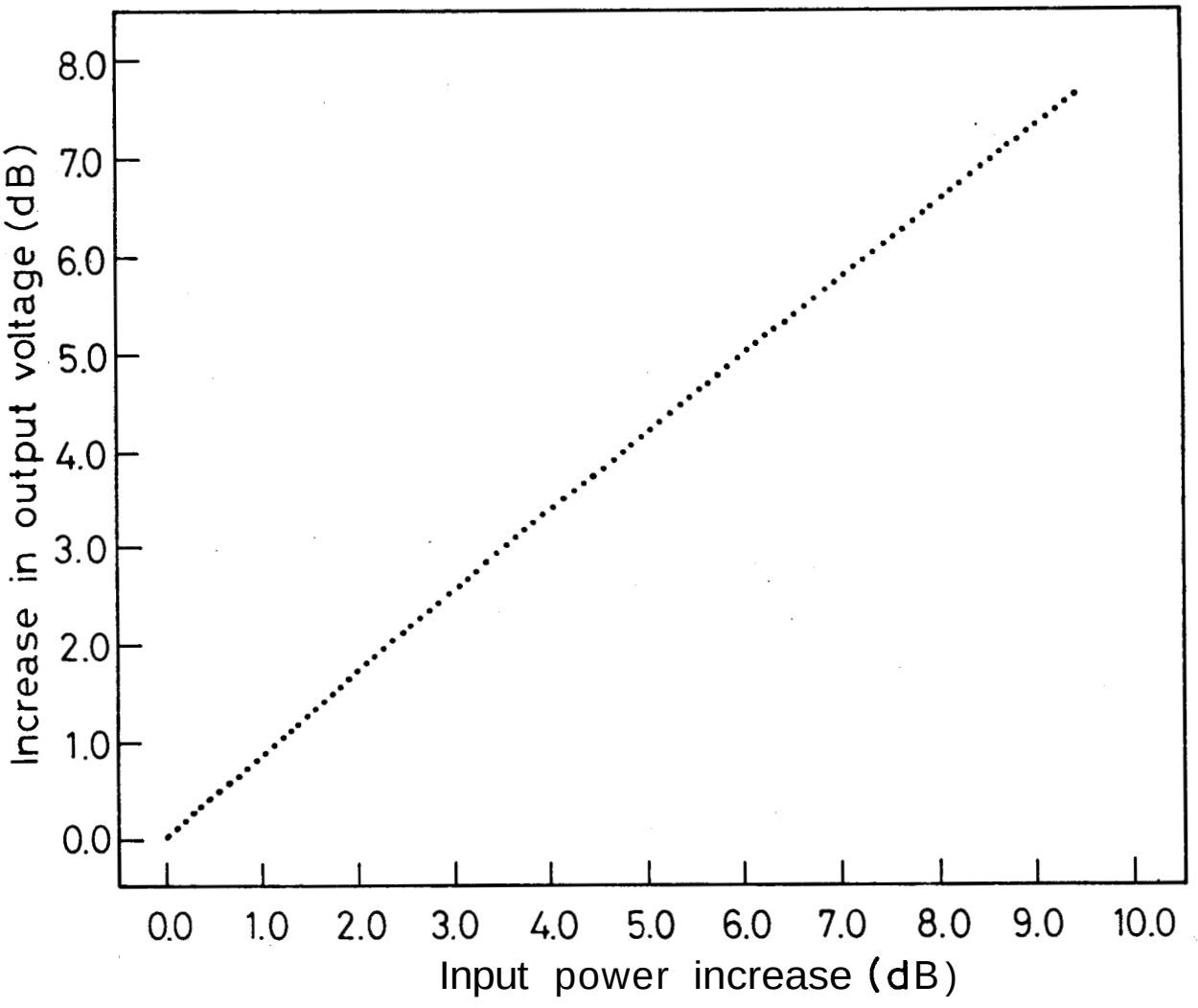

Fig. 3.3 The total power detector law (Beam 7)
slope = (1/1.28)

Janskys.

The quantity T_{Atp} was measured using several of the calibration sources. The measured values were in the range 1.3 to 1.7 with a mean of 1.5. The mean increase in system temperature per Jansky in the TP beam is therefore

$$T_{Atp} = 1.5K \text{ per Jansky}$$

The accuracy of these TP measurements depend heavily on the offsouce region chosen near the calibration source, and the stability of the system If everything is working properly then the increse in system temperautre per Jansky measured using the correlation beam and the TP beam should come out to be equal ($T_{A\phi} = T_{Atp}$). Given the kind of uncertainities that can creep into these measurements, it is satisfying that the two values agree to within 10% of each other. In what follows we adopt

$$T_{AS} = 1.5K \text{ per Jansky}$$

for the increase in system temperautre as a typical value during these observations and obtain the efficiency factors relevent to the ORT system

3.3.4 Efficiency of the ORT System

We define

$$T_{AS} = \eta T_B$$

where T_{AS} is the increase in the system temperature per Jansky and T_B is the expected main beam brightness temperature as described below. η is a factor reprasenting the overall efficiency of the ORT system

If a source of flux density S is observed with a beam of solid angle Ω_B then the beam averaged brightness temperature

T_B is given by

$$S = \frac{2k}{\lambda^2} T_B \Omega_B$$

where λ is the observing wavelength and k is the Boltzmann constant. It is assumed that the source solid angle $\Omega_s << \Omega_B$. This equation then describes a situation in which a source of flux S is spread over a sold angle Ω_B so as to have a uniform brightness temperature T over this solid angle. If this source is now observed with an ideal telescope having a main beam of size Ω_B with no sidelobes and no losses (efficiency =1) then the telescope will register an antenna temperature

$$T_A = T_B = \frac{\lambda^2}{2k} \frac{S}{\Omega_B}$$

If the ORT had a clean main beam with no side lobes and no losses in the system, then we would expect an antenna temperature T_A for a 1 Jansky source given by the above relation with as the main beam solid angle of the ORT. Ω_B was measured by taking scans across a strong point source both in the north-south and in the east-west direction and was found to be

$$\Omega_B = 6 \cdot 38 \times 10^{-5} \text{ Steradians}$$

(equivalent beam widths $\theta_\alpha = 2^\circ.2$ in e-w and $\theta_\delta = 5'.8$ in n-s for $\delta = 0^\circ$) whence the expected main beam brightness temperautre for ORT is

$$T_B = 4 \cdot 8 \text{ K}$$

Therefore

$$\eta = \frac{T_{AS}}{T_B} = \frac{1 \cdot 5}{4 \cdot 8} = 0 \cdot 31$$

The quantity η which we shall call as the overall efficiency factor will be a product of several factors which make the ORT depart from an ideal system We can write

$$\eta = \eta_B \times \eta_L \times \eta_{Tx} \times \eta_{col} \times \eta_R$$

where η_B is the main beam efficiency

η_L represents the loss in the diode phase-ahifter module

η_{Tx} represents the loss in the signal due to mismatch between the diode phase-shifter module and the RF amplifier.

%,,represents the loss due to bandwidth decorrelation because of uncompensated delays in the system

η_R represents the loss due to rms amplitude and phase errors in the system due to quantized phase shifters and errors in cable lenghths.

The value of η will increase or decrease depending on whether the value of T_{sys} is higher or lower than our estimate of 250K. Therefore if the increase (T_s) in the system temperature due to a hot region in the sky is measured employing equation 3.3, then the true beam averaged brightness temperature of the region will be given by

$$T_B = \frac{T_s}{\eta} \qquad (3.4)$$

Therefore the quantity η gives us a factor which can be used for direct conversion of an observed increase in system temperature to a beam averaged brightness temperature.

3.3.5 ORT System Noise in Units of Apparent Brightness Temperature and Apparent Flux Density

It is convenient and often desirable to represent the system noise when the antenna is pointed to a cold region in the sky, in units of apparent brightness temperature and apparent flux density (see e.g. Ball 1976). We shall denote these quantities by T_{Bsys} and S_{sys}. If the system noise is represented in these

units, then the apparent brightness temperature or the apparent flux density of any source can be obtained directly from the measured increase in system noise level when the antenna is pointed towards the source.

The true brightness temperature is equal to the apparent brightness temperature for any source whose angular structure is not smeared by the antenna beam, i.e. for a source that is completely resolved. The true flux density is equal to the peak apparent flux density for any source that is completely unresolved, i.e. small compared with the antenna beam

If an extended radio source of known brightness temperature is available for calibration then the system noise can be measured in apparent brightness temperature units directly. However even a point calibration source can be used for this purpose by converting the flux density S of the source into the units of apprent brightness temperature using the relation

$$T_{BS} = \frac{\lambda^2}{2k} \cdot \frac{S}{\Omega_B}$$

With the ORT beam, for a 1 Jansky source we get

$$T_{BS} = 4.8\ K$$

The rms noise at the output of the phase-switch beam when the antenna is pointed to a cold region is given by

$$\Delta T_{Brms} = \frac{1.414 \times T_{BSys}}{\sqrt{B\tau}}$$

If the signal to noise ratio for a 1Jansky source is 9 (see 3.3.2) then

$$\frac{T_{BS}}{\Delta T_{Brms}} = 9$$

Using B = 4MHz and τ = 1second, from the above three equations the QRT system temperature in apparent brightness temperautre

units can be calculated. We get

$$T_{Bsys} = 754\ K$$

If the signal to noise ratio for a 1Jansky source is 10 then T_{Bsys} = 678K. We can use similar relations to get the system noise S_{sys} in apparent flux density units

$$\Delta S_{rms} = \frac{1{\cdot}414 \times S_{sys}}{\sqrt{B\tau}}$$

for a 1Janksy source

$$\frac{S}{\Delta S_{rms}} = 9 \quad ; \quad S_{sys} = 157\ Jansky$$

If the signal to noise ratio is 10 then S_{sys} 141 Jansky.

The brightness temperature at 327MHz at some positions of the galactic plane averaged over the ORT beam is about 650-750K. Therefore when the antenna is moved from a cold region in the sky to one such position in the plane, then the sytem noise is expected to double (i.e. a increase by 3dB). Actual measurements also show that a 3dB increase in the system noise occurs when the antenn is pointed towards the galactic plane.

If a measurement such as described in section 3.3.2 is made towards a source using the TP beam, then the apparent brightness temperature of the source T_{BS} can be obtained using equation 3.3 by replacing T_{sys} by T_{Bsys}.

3.3.6 Effective Area of the ORT

If A_{eff} is the effective collecting area of the telescope then a source of flux density S produces an antenna temperature T_A given by

$$\frac{1}{2} S A_{eff} = k T_A$$

The factor 1/2 is because only one polarization in received by the antennna. As shown before, for a source of 1 Jansky the increase in system temperature of ORT is

$$T_A = 1.5\,K \text{ per Jansky}$$

Using this number we eastimate the effective area of ORT as

$$A_{eff} = \frac{2k}{S} \times 1.5 = 4140 \text{ Sq. meters}$$

This effective area takes into account all the factors that cause a loss in the signal from the antenna, which were discussed earlier. The A_{eff} will be larger if our value of the system temperature (T_{sys} =250K) is an underestimate. It must be mentioned here that in this way of looking at the effective area we have included all the errors in the system in the quantity A_{eff}. Strictly speaking the losses in the feed system and the mismatches only add to the system temperature and do not decrease the effective area; Phase errors in the system while causing a loss in the signal contribute to the loss of beam efficiency. However absorbing all these into the effective area calculation, gives us a quantity which is useful for calculating the senstivity of the system for certain types of measurements.

3.4 SPECTRAL LINE RECEIVERS

A spectral line in radio astronomy will appear as an increase in the system noise over a narrow range of frequencies within the total frequency band of the system In order to observe a spectral line one needs a number of receivers (usually refered to as channels) operating at adjacent frequencies and covering a narrow band centered at the frequency of the spectral line. The frequency width of each of these channels and the number of such channels required is determined by the width and extent of the spectral line being observed. It is usually good practice to have sufficient number of channels to cover a

reasonable stretch of frequencies on either side of the spectral line in order to get a good baseline.

In a simplified sense, a plot of the intensity of the signal (or the increase in system temperature) recorded in each of these channels as a function of their centre frequency gives the spectral line profile. In general however, there is more to a spectral line receiver than this simplified picture. This will be discussed later.

A possible 100 channel spectral line receiver for the ORT with a frequency resolution of 5KHz and covering a band of 500KHz is schematically shown in figure 3.4. A spectral line of interest is expected at a frequency f_{RF}. This frequency is down converted so that the line appears at an IF of f_{IF1} (=30MHz), using a first local oscillator frequency given by

$$f_{LO1} = f_{RF} - f_{IF1}$$

It is convenient to further heterodyne this signal, using a second local oscillator f_{LO2} to a second IF of f_{IF2}. The second IF (f_{IF2}) is chosen because it is usually easy to design and build narrow bandpass filters centered around a lower frequency. The choice of number of channels, frequencies f_{IF1} and f_{IF2} and the centre frequencies of the bank of filters, in fig 3.3, is only for illustration and the actual frequencies will depend on practical considerations.

The output from the final IF amplifier (centered at f_{IF2}) is split equally into 100 parts and passed through a bank of 100 filters each of width 5KHz and centered at adjacent frequencies (f1, f2,... f100) seperated by 5KHz. The outputs of these filters are detected and recorded separately. A plot of the intensity of the signal recorded in these channels against their effective centre frequency translated to RF (given by $f_i + f_{LO2} + f_{LO1}$) gives the observed spectrum In actual practice to obtain the final spectrum, a reference spectrum is measured in a band

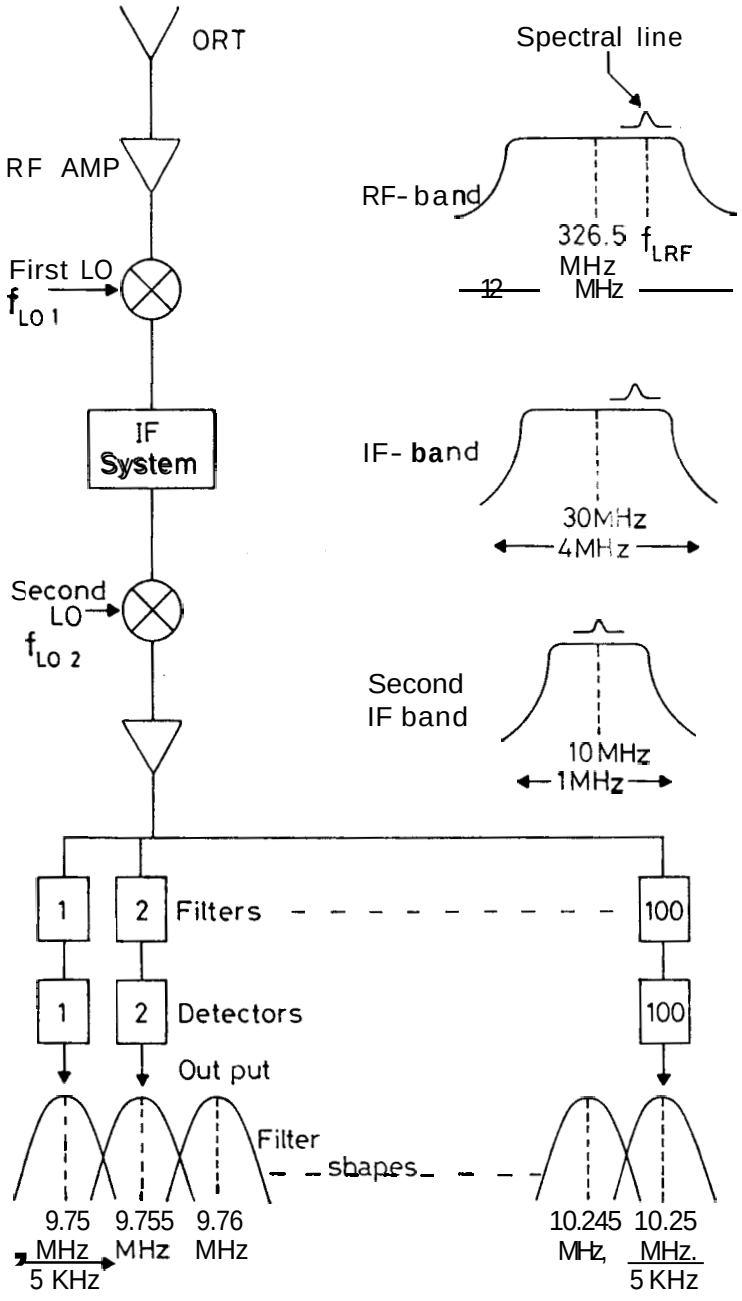

Fig. *3.4* **A possible filter-bank spectrometer for the ORT**

where the spectral line is absent, or towards an off-source region and subtracted fromthe on-source spectrum (where the line is present). The necessity of a reference spectrum and the schemes employed for measuring it will be discussed later.

It is clear from fig 3.4 that a spectral line appearing at any frequency f_{RF} within the RF amplifier band can be placed at the actual frequency band of the filter bank by choosing an appropriate first local oscillator frequency f_{LO1}. By the same token, a reference spectrum where the line is absent can be measured using the same setup by choosing another appropriate frequency for f_{LO1}. The first local oscillator is therefore an important constituent of a spectral line receiver. Its required characteristics and other functions will be discussed in section 3.6.3.

3.5 AUTOCORRELATION SPECTROMETER:

A spectral line receiver such as described in the previous section is known as the 'filter-bank spectrometer' a term which is self explanatory. The same result can be achieved using another method in 'autocorrelation spectrometers'.

3.5.1 The Method

This method makes use of a theorem in signal processing, known as the Wiener-Khintchin theorm, according to which the power spectrum of a signal is the fourier transform of its autocorrelation function. The theory of this method as applied to spectral analysis of radio astronomical signals has been discussed in detail by Weinreb (1962). We give here a summary of the principles of this method

Let x(t) reprasent a signal as a function of time, whose power spectrum is P(f). The autocorrelation function of x(t) is defined as

$$(\tau) = \lim \frac{1}{2T} \int_{-T}^{T} x(t).\, x(t+\tau)\, dt \qquad (3.5)$$

$R(\tau)$ is the time average of the signal multiplied by a delayed replica of itself. The power spectrum is then given by

$$P(f) = 2\int_{-\infty}^{\infty} R(\tau)\, e^{-j2\pi f\tau}\, d\tau$$

The operations indicated in equations 3.5 and 3.6 cannot be performed in practice; an infinite segment of $x(t)$ and an infinite amount of apparatus would be required. However it is sufficient to measure $R(\tau)$ form $-\tau_{max}$ to $+\tau_{max}$, in which case one obtains a frequency resolution in the power spectrum of the order of $1/\tau_{max}$. Further simplifications are also possible. It is clear that $R(\tau)$ is a symmetric function about $\tau = 0$, i.e $R(\tau) = R(-\tau)$. This cuts down the range of τ over which the measurements have to be made to one half. Further it is shown below that it is sufficient to measure $R(\tau)$ at only discrete points at equal intervals.

Another theorem in signal processing which is made use of in the practical realization of this type of spectrometer is the Nyquist sampling theorem If the signal $x(t)$ is band limited such that its power spectrum $P(f) = 0$ for $f > f_{max}$ then, according to this theorem, in order to recover all the properties of this signal (for example $P(f)$) it is sufficient to record the samples of this signal at discrete intervals separated by a time $\Delta t = 1/2f_{max}$ (the sampling frequency $f_s = 2f_{max}$). Therefore the bandlimited signal $x(t)$ can be represented as $x(k\Delta t)$, $k = 1, 2, 3 \ldots (K+N)$, where $(K+N)$ is the total number of samples.

We can now write the equivalent of equation 3.5 in discrete form for a limited number of samples as

$$R(n\Delta\tau) = \frac{1}{k}\sum_{k=1}^{K} x(k\Delta t).\, x(k\Delta t + n\Delta\tau) \qquad (3.7)$$

The autocorrelation function is measured up to a $\tau_{max} = (N-1)\Delta\tau$. The spectral estimate $P(i\delta f)$ is calculated using the discrete fourier transform

$$P(i\delta f) = 4\Delta\tau \sum_{n=0}^{N-1} R(n\Delta\tau)\, w(n\Delta\tau) \cos(2\pi\delta f n\Delta\tau) \qquad (3.8)$$

The numbers $w(n\Delta\tau)$ are samples of a weighting function which must be chosen. The weighting function must be even and have $w(\tau)=0$ for $\tau >$ NAY. The significance of $w(\tau)$ is discussed later. $P(i\delta f)$ is the discrete power spectrum of the signal. From equation 3.8 it is the fourier transform of the function $R(n\Delta\tau)$ which is band limited to $(N-1)\Delta\tau$. Therefore according to the Nyquist sampling theorem, δf must be chosen equal to $1/[2(N-1)\Delta\tau]$ in order to use all of the information contained in $R(n\Delta\tau)$. δf is the separation between adjacent points in the spectrum.

As the autocorrelation function is measured only up to $\tau_{max}=(N-1)\Delta\tau$, the frequency resolution of the spectrum (Δf) is of the order of $1/[(N-1)\Delta\tau]$. The actual frequency resolution Δf depends on the choice of the weighting function $w(\tau)$. The restriction on $w(\tau)$ is that it be zero for $\tau > N\Delta\tau$, as the autocorrelation function is not measured in this range. The weighting funcion $w(\tau)$ is exactly analogous to the grading function of a filled aperture antenna. The fourier transform of the grading function gives the angular beam pattern of the antenna. Similarly the fourier transform of the weighting function gives the effective filter shape which convolves the true spectrum of the signal, being analysed. The choice of $w(\tau)$ is usually a compromise between obtaining a filter with a norrow main lobe and high spurious side lobes or a filter with a broadened main lobe and low spurious lobes. Usually a cosine weighting function also known as the Hanning weighting function is used. It is given by

$$W(n\Delta\tau) = 0.5 + 0.5\cos\frac{\pi n}{N} \quad \text{for } |n| < N$$
$$= 0 \quad \text{for } |n| \geq N \qquad (3.9)$$

This gives a frequency resolution of $\Delta f = f_s/N$ and spurious responses are 16dB below the main response. A uniform weighting function defined by

$$W(n\Delta\tau) = 1 \quad \text{for } |n| < N$$
$$= 0 \quad \text{for } |n| \geq N$$

gives a $(\sin x/x)^2$ pattern with half power width $\Delta f = 0.604 f_s/N$ and the spurious response is at -7dB level.

In practice it is convenient to perform the operation indicated in equation 2.7 using digital hardware and the modified fourier transform operation (equation 2.8) using the fast fourier transform (FFT) algorithm on a computer. In order to achieve this the samples $x(k\Delta t)$ are usually digitized in an A/D converter. The number of bits used for digitization depends on the accuracy of the results desired and the complexity of the hardware one is willing to build. In the extreme case, the digitization can be reduced to a one-bit level, in which case the hardware required is enormously simplified. Later in this chapter we will describe and discuss one such 1-bit autocoreelator built and installed as a backend spectral line receiver for the ORT, and used for the observations reported in this thesis.

A possible hardware scheme for implementing the operation indicated in equation 3.6 is shown in fig 3.5. This scheme achieves essentially the same result as the filter bank method in fig 3.4. The second IF in fig 3.5 has to be a 'video' band going from 0 to f_{max} in order to meet the requirement that $x(t)$ be band limited ($P(f)=0$ for $f > f_{max}$). In principle, the actual second IF band can extend from $2nf_{max}$ to $(2n+1)f_{max}$ (where n is an integer, 0 inclusive) to achieve the same result with exactly the same scheme, as in fig 3.5. This is because the discrete sampling of the signal at intervals $\Delta t = 1/f_s$ is equivalent to a filter with responses at multiples of the sampling frequency f_s. In most proctical cases, however, it is convenient to have the signal extend from 0 to $f_s/2$ ($=f_{max}$). It may be noted that the sampling frequency cannot be less than $2f_{max}$, otherwise aliasing will occur; frequencies beyond $f_s/2$ will be folded over.

The second IF band extending from 0 to f_{max} at the output of the low pass filter in fig 3.5 is folded about the second LO frequency; the bands IF1 (=30MHz) to $(IF1-f_{max})$ and IF1 to $(IF1+f_{max})$ are folded into the same band (0 to f_{max}). This band

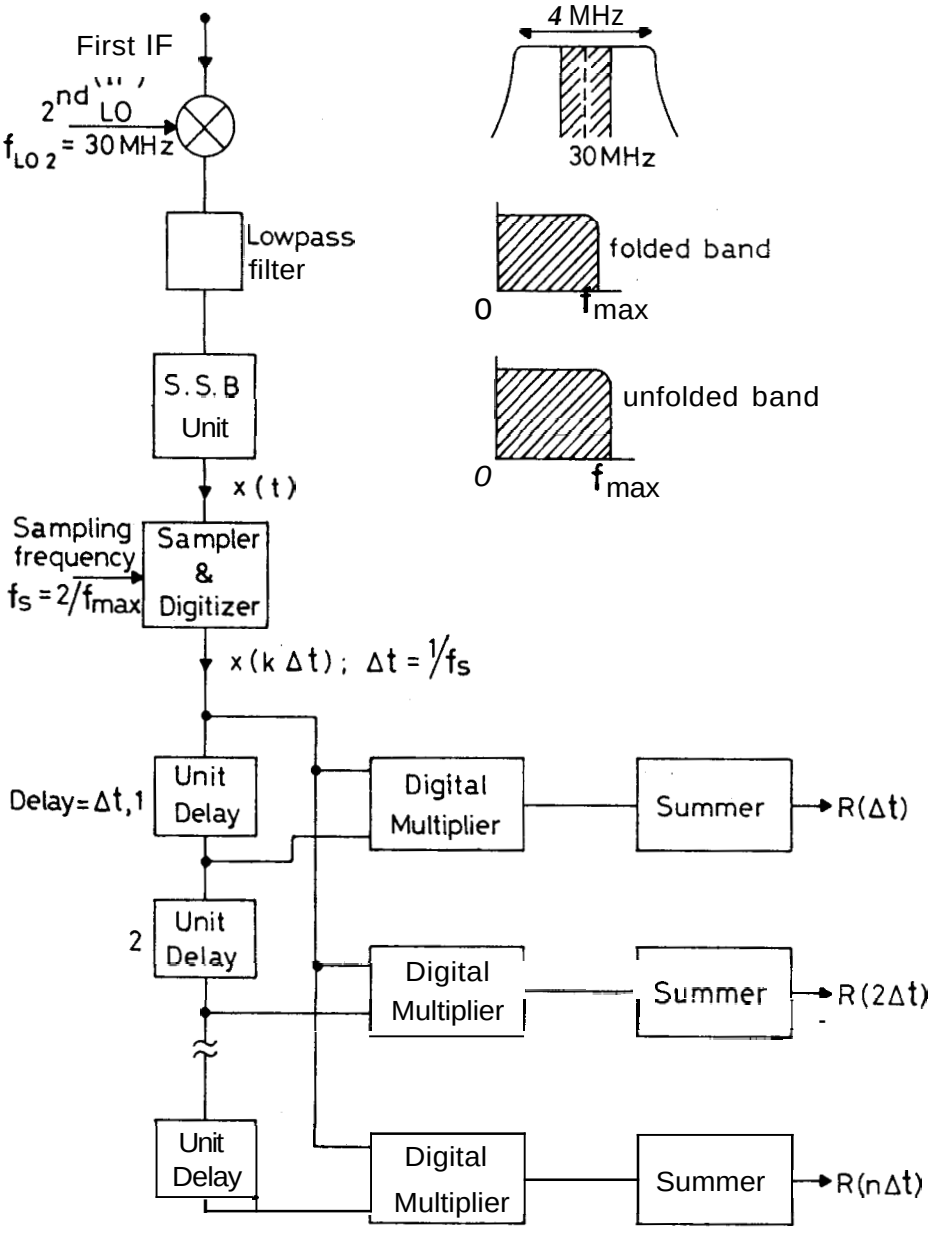

Fig. 3.5 A typical digital autocorrelation spectrometer.

can be unfolded using standard single sideband techniques (the SSB unit of fig 3.5). The output of the SSB unit is then our signal $x(t)$ which is bandlimited to f_{max}. This is sampled at a frequency $f = 2f_{max}$ and digitized. The train of samples $x(k\Delta t)$ goes through the hardware which computes the autocorrelation function $R(n\Delta t)$ as shown in fig 3.5.

As the autocorrelation function is a real and symmetric function the power spectrum can be computed using a simple cosine descrete transform given by

$$P(i\delta f) = 4\Delta t \sum_{n=0}^{N-1} R(n\Delta t)\, W(n\Delta t)\, \cos(2\pi i \delta f n \Delta t) \qquad (3.10)$$

An appropriate weighting function $w(\tau)$ (such as in eqn 3.9) is chosen to get the desired frequency resolution Δf, with the restriction that $\Delta f > 1/[(N-1)\Delta t]$.

3.5.2 Advantages of the Autocorrelation Method

The stability of a digital autocorrelaion spectrometer is much superior compared to a filter bank spectrometer. In the latter the different filters of the spectrometer can (and in general will) have different gains and different variations of gain as function of time. This can introduce uncertainities in the measured spectrum unless extreme care is excercised. Further the differences in the 'laws' of the detectors at the output of different filters have to be made as small as possible for satisfactory performance. Any differences should be calibrated and taken into account in the final measurement, particularly when one is trying to achieve rms noise levels of order of 10^{-3} to 10^{-4} of the total system temperature. In a digital autocorrelator this problem is practically absent. Any gain variations in the system uniformly affects all the channels and there are no differential variations. It is usually easy to take out the uniform variations by proper measurement of a reference spectrum

The major advantage of an autocorrelation spectrometer is its flexibility for obtaining different frequency resolutions and total bandwidths. Practically any frequency resolution and total bandwidth can be obtained by just changing one or two components of the whole system. A change in the cutoff frequency (f_c) of the low pass filter in fig 3.5 changes the total band width of the system Only the sampling frequency has to changed to accommodate this change in the bandwidth. The frequency resolution of the spectrometer is given by

$$\Delta f = \frac{f_s}{N} \quad \text{with the restriction that} \quad f_s \geq 2 f_{max}$$

The resolution can therefore be changed by merely changing the sampling frequency f_s. However, when $f_s > 2B$ there is a reduction in the total number of channels where useful signal is present; some of the channels will record the signals in the stopband of the low pass filter.

3.6 A ONE-BIT AUTOCORRELATION SPECTROMETER FOR THE ORT:

The spectral line back-end used for the recombination line observations reported in this thesis is a 128-channel one-bit autocorrelation spectrometer. In this section we discuss the details of the set up of this instrument for spectral line observations.

3.6.1 Principle of the 1-bit Method

According to the Nyquist sampling theorem all the information contained in a signal $x(t)$, bandlimited to f_{max}, can be recovered by sampling it at a freqeuncy $f_s \geq 2f_{max}$. The signal is then represented by $x(k\Delta t)$ whete $t = 1/f_s$, $k=0, 1, 2....$ For further processing of this signal $x(k\Delta t)$ is digitized. The digitization can be carried out to the extreme level, namely to 1-bit where only the sign of the signal is recorded. Then according to a theorem due to Van-Vleck and Middleton(1966) it is still possible to recover the information about the spectral

content of the signal. The theorem can be stated as follows

Suppose that x(t) is a gaussian random signal with zero mean and y(t) is formed by one-bitting or infinite clipping of x(t), that is

$$y(t) = 1 \text{ when } x(t) \geq 0$$

and $y(t) = -1$ when $x(t) < 0$

then the normalized autocorrelation functions of x(t) and y(t) are related by

$$\rho_x(\tau) = \sin\left(\frac{\pi}{2}\rho_y(\tau)\right) \qquad (3.11)$$

This equation is valid for the normalized autocorrelation function given by

$$\rho(\tau) = \frac{R(\tau)}{R(0)}$$

where $R(\tau)$ is as defined in equation 3.7. Equation 3.11 is known as the Van-Vleck correction and it is valid only for certain classes of signals, such as those arising from gaussian random processes. Most signals in radio astronomy fall into this class. The Van-Vleck correction is also valid for a single sinewave and also approximately true for a weak sinewave in a gaussian noise.

In the digital method $\rho_y(\tau)$ is now computed as

$$\rho_y(n\Delta t) = \frac{1}{N}\sum_{k=1}^{N} y(k\Delta t)\, y(k\Delta t + n\Delta\tau) \qquad (3.12)$$

Because of the simple nature of y(t), every term in the summation in equation 3.12 has a value +1 or -1. The operation indicated in this equation can be performed using extremely simple digital circuits.

The sampler and digitizer in fig 3.5 can now be replaced by a zero cross detector and a gate. The unit delays can be obtained in shift registers ; for N channels one needs an N-bit shift register. The multiplication is now reduced to coincidence

detection which can be done using exclusive OR gates. The summation can be performed using simple counters.

There is always a price one has to pay for such simplification. There are two things that happen in this case. One is that due to clipping all the information about the absolute amplitude of the input signal is lost. The fourier transform of the Van-Vleck corrected autocorrelaion function $\rho_x(\tau)$ gives only a **normalized** power spectrum To obtain the actual '**scale**' for the spectrum it has to be **supplimented** by a separate measurement of the total power of the signal going into the system This is usually done by making a measurement of the on-source system temperature.

Secondly, there will be a degradation of the signal to noise ratio of the spectrum as compared to a many-bit or an analog system For an analog system the **rms** noise temperature at the output of each channel is given by

$$\Delta T_{rms} = \frac{T_{sys}}{\sqrt{\Delta f \cdot t}}$$

where Δf is the frequency resolution and t is the integration time. Weinreb (1962) has shown that for 1-bit digital autocorrelation spectrometer the **rms** noise is given by

$$\Delta T_{rms} = \alpha \cdot \beta \cdot \frac{T_{sys}}{\sqrt{\Delta f . t}} \sqrt{1 - \frac{\Delta f}{b}} \qquad (3.13)$$

where b is the total bandwidth of **the** spectrum being analysed. α **is** a factor close to unity and **it** depends on the weighting function $w(\tau)$ used. For cosine weighting (**eqn** 3.9) $\alpha = 0.866$ and for uniform weighting $\alpha = 1.099$. β reprasents the increase in the noise due to one-bitting. Its value depends on the exact shape of the filter used for bandlimiting the signal **x(t)**. For a rectangular **bandpass** the theoretical value of is $\pi/2$.

The operations performed in a one-bit autorrelation

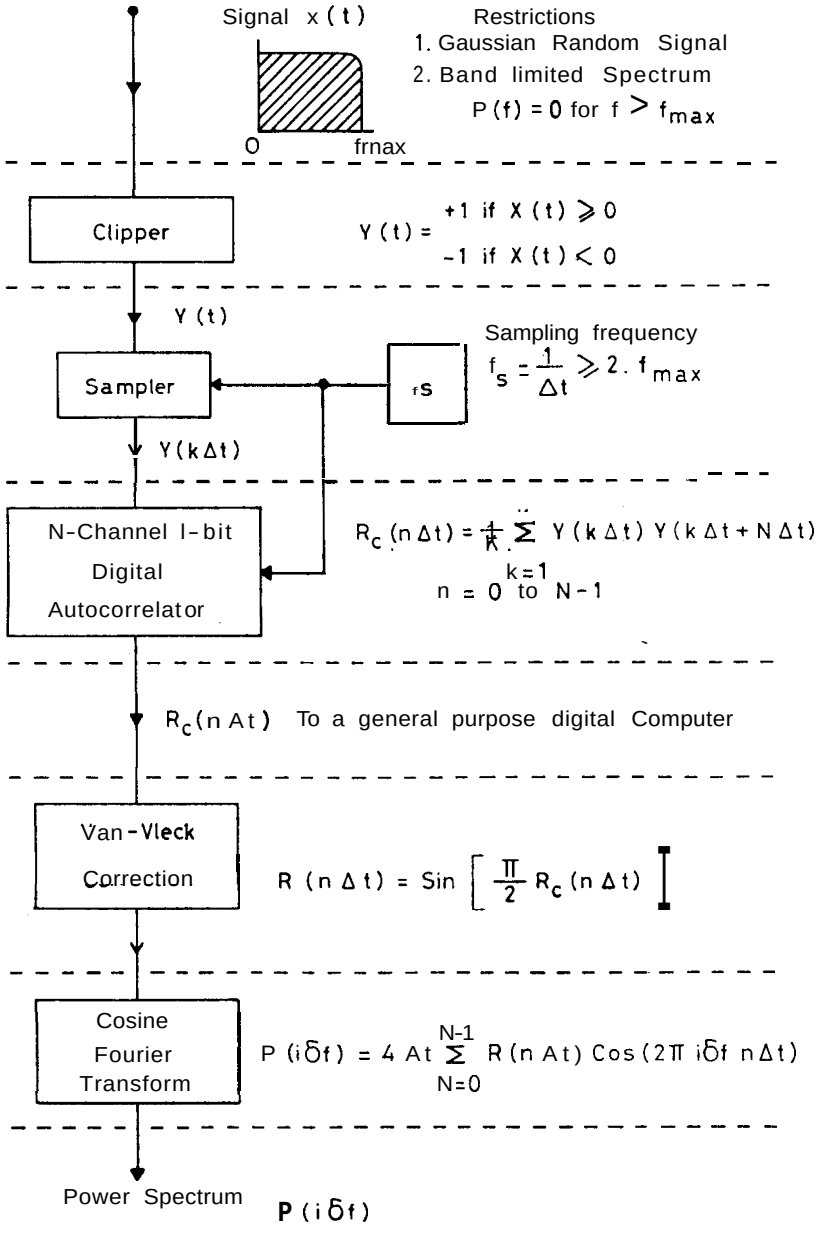

Fig. 3.6 Sequence of operations in a 1-bit digital autocorrelator.

spectrometer are shown in the block diagram fig 3.6.

3.6.2 Front-end Analog System

A block diagram of the overall receiver system for spectral line observations is shown in fig 3.7a. Any narrow frequency band within the total bandwidth of the ORT (shaded area in fig 3.7a) is translated to the first IF band at 30MHz using the first local oscillator. This signal taken from the ORT beam 7 output is translated to the video band (0 to f_{max}) in the front end analog system A standard single sideband (SSB) technique is used to achieve this.

The signal level entering the SSB unit is monitored in a separ'ate branch using a detector and a current meter as shown in fig 3.7b. The SSB technique is illustrated in fig 3.8. The two mixers' A and B are operated with local oscillators in quadrature and at the centre of the input band (=30MHz). The quadrature shifted local oscillator for mixer A rotates the phase of the upper and lower sidebands by -90° and $+90^{\circ}$ respectively with respect to the output from mixer B. At the outputs of mixers A and B the upper and lower sidebands are folded. An additional 90° phase shift is applied to the folded band at the output of mixer A. This shift will make the phase of the upper side hand come back to the same phase as at the output of mixer B. But the lower sideband will now have a phase shift of 180° with respect to the output at mixer B. An addition of the two folded bands will therefore cancel the lower sideband. A subtraction would have cancelled the upper sideband.

The actual implementation of the SSB technique is shown in fig 3.8b. The 90° phase shift required in one of the arms is achieved using another local oscillator at 1MHz. Since the rejection of the unwanted sideband depends on the exact phaseshift between the two arms and also the amplitude characteristics of the two arms , mixers having the same gain and identical filters are used in the two arms. The second 1MHz local oscillator is fig 3.8b removes the band inversion caused by

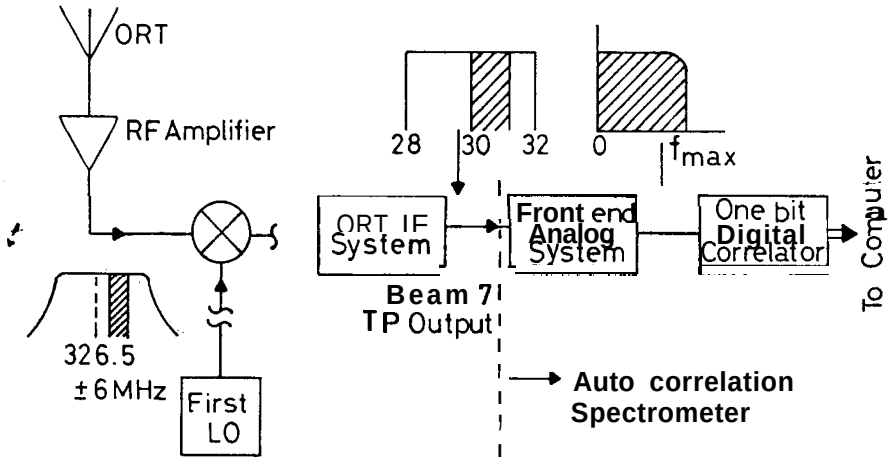

Fig. 3.7a A block diagram of the complete system for line observations.

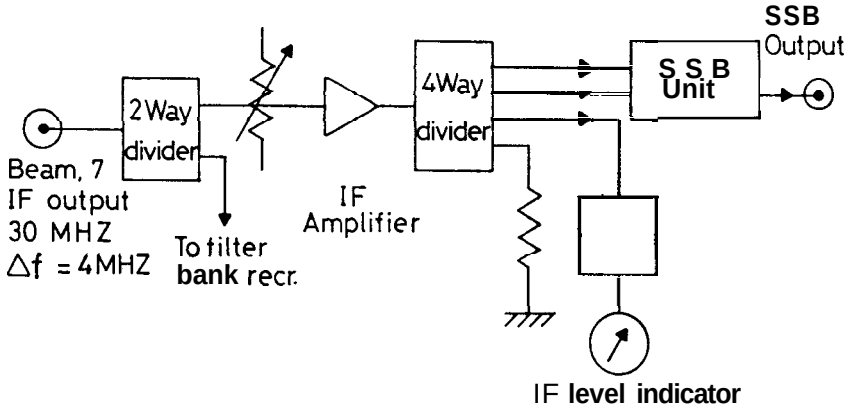

Fig. 3.7b Signal flow for the line receiver.

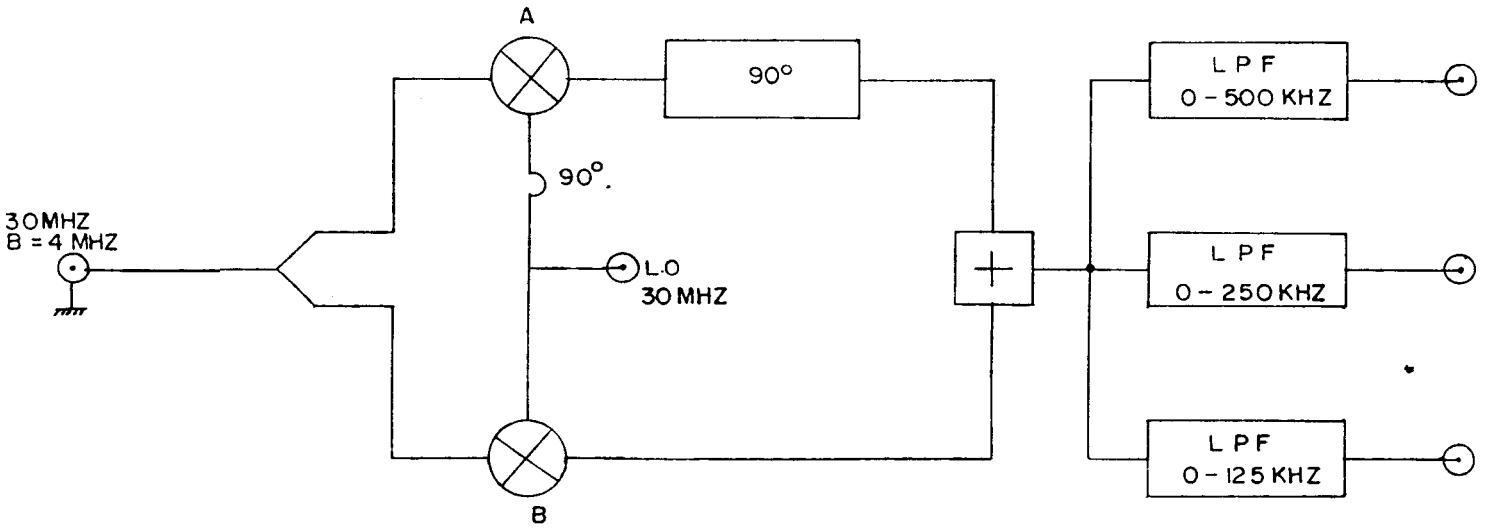

Fig. 3.8a The single side band (SSB) technique and the low pass filters for the front end.

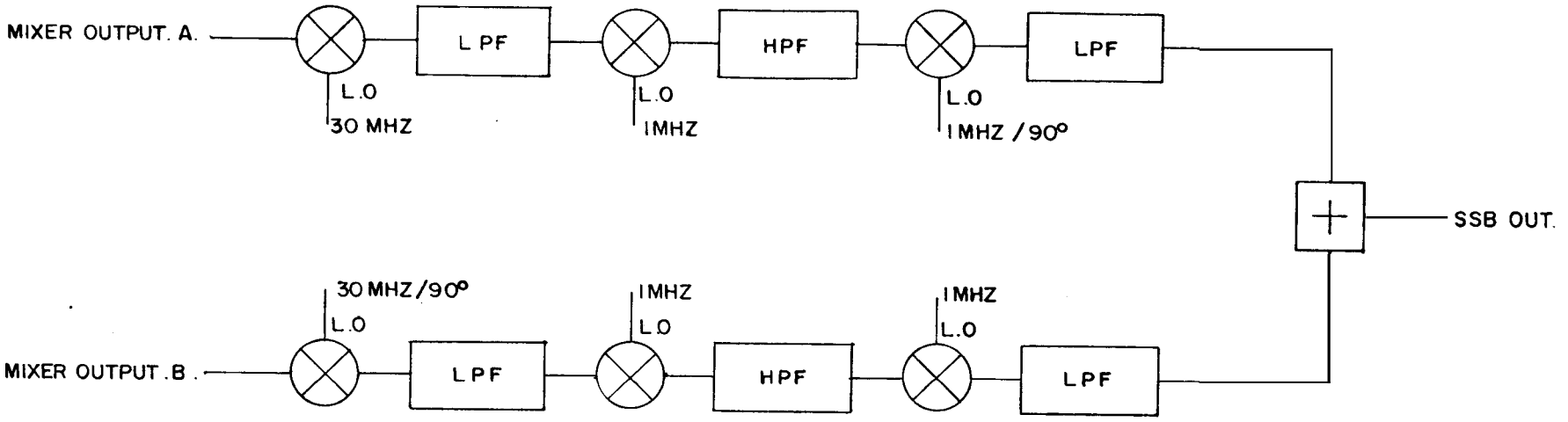

Fig. 3.8b Implementation of the SSB technique 1MHz LOs are used to obtain the 90° phase shift.

the first 1MHz LO. The system gives better than 25dB rejection of the unwanted sideband over the video frequency range of 30KHz-800KHz.

Three video filters of bandwidths 500KHz, 250KHz and 125KHz are provided at the output of the SSB unit. Any one of these filters can be selected using a front panel bandswitch.

3.6.3 The First Local Oscillator

As mentioned in section 3.4 the first local oscillator (FLO) (fig 3.4 and 3.6) is an important constituent of the spectral line receiver. By choosing an appropriate frequency for the FLO a required band at the RF can be brought down to the final IF band analysed by the spectrometer.

There are several requirements to be met by the FLO system Its frequency should be accurate as it determines the exact effective frequencies of the different channels of the spectrometer. The output LO signal should be spectrally pure ; any spurious frequencies should in general be better than 30dB below. As will be discussed later (see chapter 4) for spectral line observations it is necessary to be able to switch the FLO between 2 or 3 frequencies at a fast rate. The settling time for the switched frequency should be as small as possible (usually of the order of milliseconds). It should be possible to set any frequency from a remote control (usually a computer).

A block diagram of the FLO system employed for the ORT spectral line receiver is shown in fig 3.9a. A frequency synthesizer employing a direct synthesis technique derives the required frequencies from a highly stable 1MHz reference obtained from a rubidium frequency standard. A description of the synthesis technique adopted can be found in Ravindra et al (1976). The frequencies generated are in the range 8.1067MHz to 8.3192MHz in steps of 0.833KHz. These frequencies after multiplication by a factor of 36 gives the required LO frequencies in the range 291.84MHz to 299.49MHz in steps of

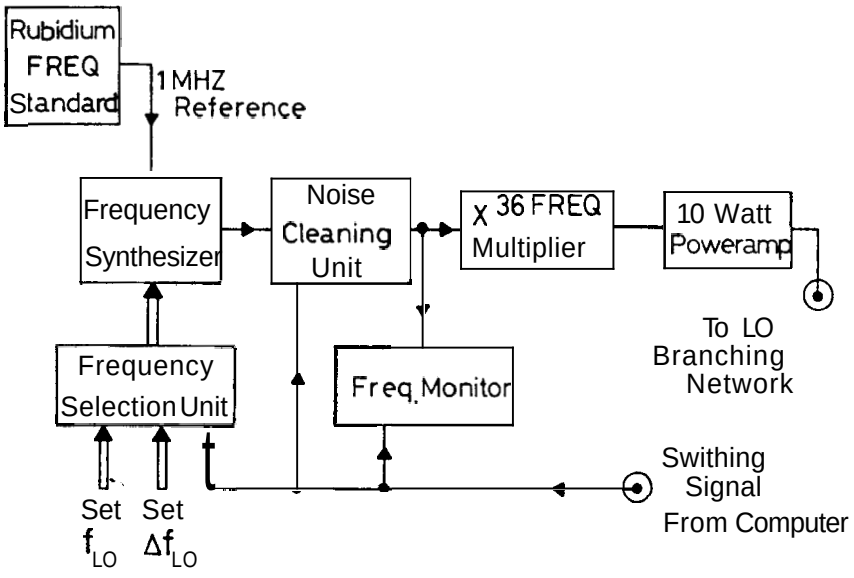

Fig. 3.9a A Block diagram of the first local oscillator system.

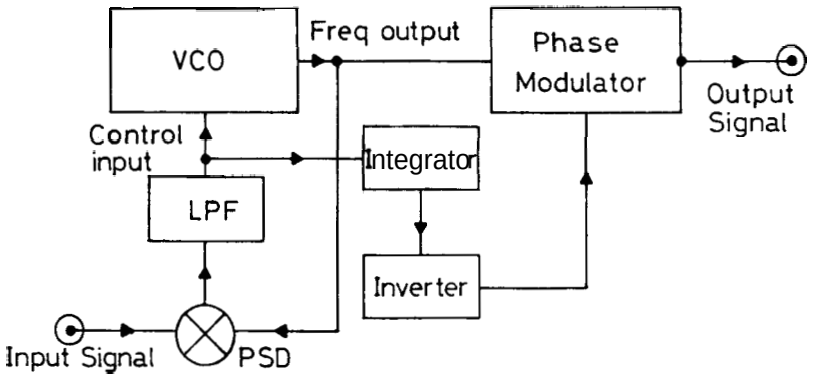

Fig. 3.9b The noise cleaning unit for the local oscillator.

30KHz.

Any required frequency (f_{LO}) in this range and an offset (Δf_{LO}) can be set using the frequency selection unit. A square wave switching signal coming from the computer will switch the frequency of the synthesizer between f_{LO} and ($f_{LO} + \Delta f_{LO}$). Through a front panel switch it is possible to select any one of the following 4 modes of switching

1. No switching
2. Switch between f_{LO} and $f_{LO} + \Delta f_{LO}$ (REF1)
3. Switch between f_{LO} and $f_{LO} - \Delta f_{LO}$ (REF21
4. Switch between all 3 in the sequence f_{LO}-REF1-f_{LO}-REF2-f_{LO} etc

These modes are convenient for spectral line observations employing single or double frequency switching schemes.

A frequency counter monitors the frequency of the synthesizer. Although the counter operates at the synthesizer frequency of around 8MHz, the actual frequency counted is displayed after multiplication by 36 in order to show the exact final LO frequency. During frequency switching the counter displays the switched freqeuncies in that sequence.

As mentioned eerliar the LO frequency should be of high spectral purity. Generally, in direct frequency synthesis, spurious frequencies are always present at the output. In the frequency synthesizer that was builtfor these observations (Ravindra et al 1976), these spurious frequencies were about 30dB below the level of the desired frequency. The spurious frequencies are usually present at the output as frequency or phase modulation. A multiplication by a factor of 36 will increase the level of the spurious frequencies by 30dB; multiplication by n increases the spurious level by n^2. Therefore if the output of the synthesizer were directly multiplied then the spectral purity of the LO would be completely lost. For this reson a noise cleaning unit which suppresses the spurious frequencies by an additional 20-25 dB was inserted between the frequency synthesizer and the multiplier

The noise cleaning unit has some novel features. Spurious frequencies which are farther than about 2KHz are first suppressed to better than 60dB in a phase locked loop as shown in fig 3.9b. The loop bandwidth has to be kept sufficiently large so that the settling time for the loop in the switched frequency mode is still small. Spurious frequencies within this band are still present in the form of frequency modulation at the output of the voltage controlled oscillator (VCO). The control voltage for the VCO contains the information about these spurious frequencies. This signal is integrated to give the phase of the modulating spurious signals. The VCO output is again phase modulated using this siganl after a phase change of 180^{0}. This process antimodulates the output of the VCO and cancels the spurious frequencies present in it. The level of cancellation will depend on the phase and amplitude stability of the integrator -and the inverter. It was possible to achieve a rejection of the spurious frequencies by 20-25dB. The spurious frequencies at the final LO output after multiplication were about 20-25dB below the true frequency and are likely to show up in the measured spectrum only if the signal to noise ratio is >100.

The phases lock loop in the noise cleaning unit increase the settling time of the LO frequency in the switched mode. This time was reduced to a few milliseconds by switching the DC control voltage to the VCO at the same rate. This control voltage was derived from an 8-bit D/A converter. The same 8-bits generated by the frequency selection unit that controls the frequency of the synthesizer were used for this purpose.

3.6.4 The Digital Correlator

A block diagram of the 128 channel one-bit digital autocorrelator is shown in figure 3.10 The video signal fromthe front end analog system is converted to a I-bit signal (digital 0 if signal is negative and 1 if positive) in the zero cross detector. The one-bit signal is sampled at an appropriate sampling frequency which can be selected from a front panel

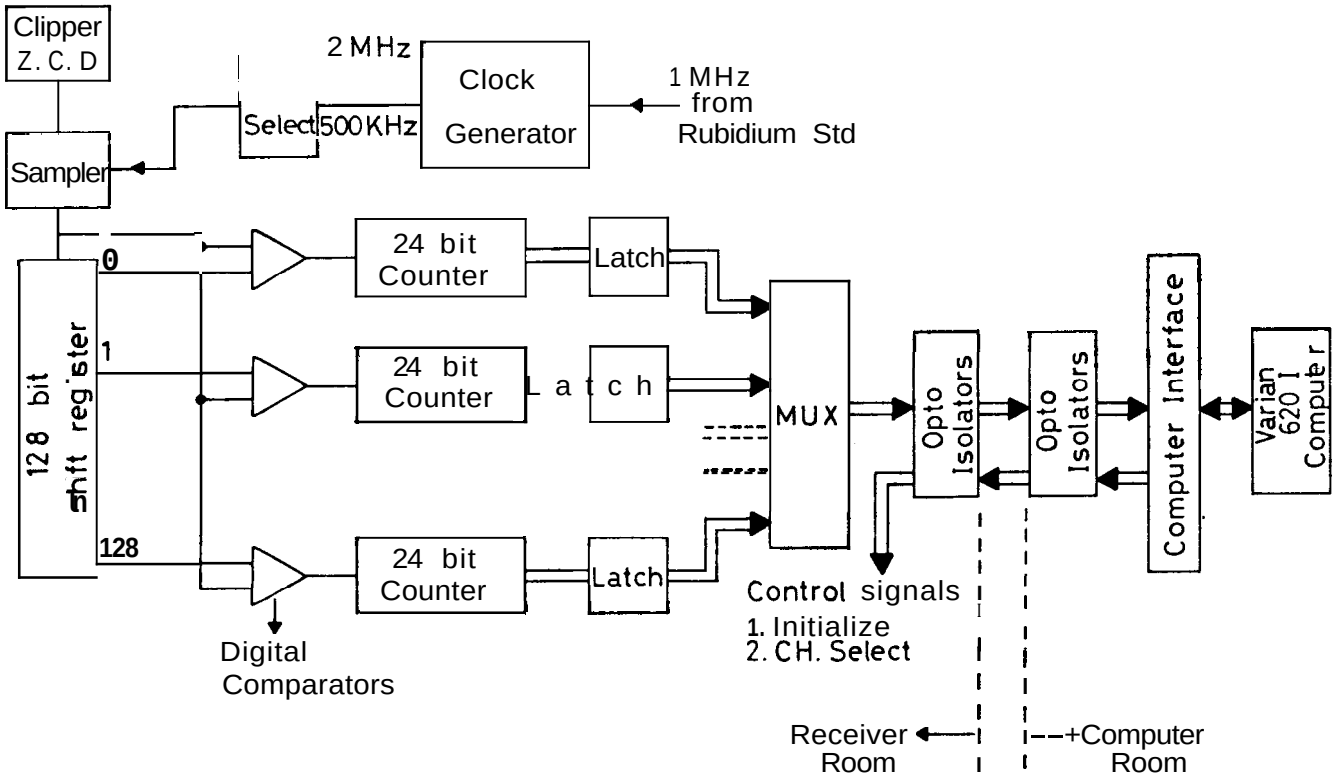

Fig. 3.10 The 1-bit digital Auto Correlator.

switch. The 128 delays are obtained .using 128-bit shift-register. Digital comparators (exclusive OR gates) are used for multiplication of the input data stream and the delayed signals. The number of coincidences are counted in 24-bit counters connected to each of the comparators. A control signal can 'latch' the counter values into the buffers and clear the counters immedietly after latching. The latched values of the 128 counters are multiplexed into a 12-bit data bus connected to the computer (Varian 620i) through a computer interface. Opto-isolators are used at either end to avoid electrical pickup in the lengthy data lines running from the correlator to the computer. CMOS integrated circuits have been used for all the operations. This restricts the maximum clock frequency to about 2MHz.

The 0 delay counter essentially counts the number of clock pulses. as it represents the multiplication of the signal with itself. The number of bits filled in this counter depends on the clock frequency (i.e. sampling frequency) and the integration time. Although the counters are 24-bits long they are essentially used as 20-bit counters (the 20 LSB's are used). Out of these 20 bits only the 12 MSB's are read by the computer. The effective bit-length of the counters M (=20 in this case) determines the maximum time T_{max} which may elapse before the counter is full and data readout must occur. Thus the T is given by

$$T_{max} = \frac{2^M - 1}{f_s} \quad ; \quad f_s = \text{Sampling frequency}$$

Reading of only the 12 MSBs of the 20-bit counter introduces a round off error. However this round off error is smaller than the rms deviation of each of the counter values which is approximately . For a typical sampling frequency of 1MHz and integration time T=0.25 seconds = 500. The 8 bits discarded will have a maximum value of 256 which only introduces a small error. This error can be further reduced if instead of discarding the 8 bits they are really rounded off and added to

the 12 bits that are read. This has been achieved in this correlator by allowing 255 extra sample pulses into the zero delay counter during every integration period.

The integration period T can be selcted internally by the correlator or externally by the computer. Four internal integration times are provided. These are the times it takes to fill 20, 19, 18 and 17 bits respectively in the zero delay counter. These integration times T1, T2, T3, and T4 are given by $(2^{M_0}-1)/f_s$ where M0=20, 19, 18, 17 respectively. These internal integration times can be selected by a front panel band switch.

At the end of each integratin period the autocorrelator generates an interrupt (INT) pulse. The occurence of this pulse causes the following sequence of actions in the correlator

1. The sampling clock is stopped
2. The counter values are latched into the buffers
3. Channel '0' is selected on to the 12-bit data bus.
4. All counters are cleared
5. Sampling clock is restarted

The INT pulse generated in the correlator is also available to the computer to initiate data readout channel by channel. A sequence of channel select pulses coming from the computer places the value of succesive counters (available in the buffers) on the data bus sequentially. The computer performs a read operation after each channel select pulse is sent. The INT pulse can also be generated and sent by the computer in which case the integration period is externally determined. The external integration time should be < T_{max} in order to avoid overflow of counters. The external integration mode can be selected using a front panel band switch.

The counters in each channel count only the number of coincidences. The counts in channel '0' give the total number of clock pulses. The normalized autocorrelation function is given by

$$\rho_4(n\Delta t) = \frac{2N_n}{N_0} - 1 \qquad (3.14)$$

Where NO is the number of counts recorded in channel '0' and N_n is the number of counts recorded in counter n

3.6.5 The Data Acquisition Software

Spectral line observations using the 1-bit correlator are carried out using data acquisition software written for the Varian 620i computer. The program can perform the following functions

1. The program accepts and records information like date, name of the source, video bandwidth used, sampling frequency, FLO setting, declination, observing duration etc.

2. Using the given LO frequency the program calculates and sets IF phases and delays for the ORT to point to the required declination.

3. For the given observing time (in multiples of one minute) the program accumulates the normalized autocorrelation function for every minute and records it on magnetc tape after applying the Van-Vleck correction. Data is recorded separately for the online and offline LO frequencies. The observing time is divided equally between the online and offline frequencies by alternately spending 250 milliseconds at each frequency. The program sends out a switching signal (a square wave of period 500ms) to the freqeuncy synthesizer to switch between the online and offline frequencies. A dead time of 10 ms is allowed after each switching for the system to settle down.

4. If required the program can set different IF phases and delays for the online and offline frequencies to compensate for the beam shift that occurs due to the change in the local oscillator frequency. (see section 4.3)

5. The program also accumulates separately the online and offline autocorrelation functions (after Van-Vleck correction) for the total observing duration. At the end of the observations fourier transforms are computed for the averaged online and offline autocorrelation functions. The observed spectrum is then computed using

$$P(n) = \frac{P_{on}(n) - P_{off}(n)}{P_{off}(n)} \qquad (3.15)$$

where $P_{on}(n)$ and $P_{off}(n)$ are the online and offline values for, the nth point in the spectrum obtained from the fourier transform. The division by $P_{off}(n)$ corrects for the input video bandshape.

6. The online and offline autocorelation functions, their fourier transforms and the observed spectrum are all plotted at the end of the observing duration, for immediate inspection.

3.6.6 The Performance of the Autocorrelation Spectrometer

Several tests have been performed to check the satisfactory functioning of the complete spectral line receiver. The 1-bit autocorrelator essentially measures the input video bandshape. The fourier transform of the measured autorcorrelation function weighted using a function such as in equation 3.9, gives the input bandshape convolved with the fourier transform of the weighting function.

With the antenna tracking an offsource region the bandshapes of the three video filter (fig 3.8a) with cutoffs at 125Hz, 250 KHz and 500KHz were measured by recording their autocorelation functions for several minutes. The autocorrelation functions were fourier transformed to get the bandshapes. The bandshapes of all the filters so measured compare well with the actual

laboratory bandshape measurements of these filters using swept frequency techniques.

The expected rms noise in the spectrum measured using the 1-bit autocorrelator can be calculated using equation 3.13. With the antenna tracking an offsource region spectra were obtained using the 500 KHZ filter (and f_s =1 MHz) for different integration times T ranging from 1 minute to several hours. Double frequency switching was used during these measurements (mode 4 as explained in 3.6.3). Equation 2.15 was used to compute the observed spectrum. The value of which represents the increase in the noise due to clipping was found to be between 1.5 and 1.6, by comparing the rms noise in the observed spectra with that expected according to equation 3.13.

One of the advantages of the 1-bit correlator is that the measurements are not sensitive to the input signal level. The correlator looks only at the zero crossings of the signal and not at its amplitude to get the spectral information. Measurements of off-source spectra were made with different input signal levels. Identical results were obtained even when the input signal level was changed by as much as 10dB.